Received April 3, 2017, accepted May 1, 2017, date of publication May 18, 2017, date of current version June 28, 2017.

Digital Object Identifier 10.1109/ACCESS.2017.2705484

A Compact V-Band Planar Gap-Coupled 4 × 1 Antenna Array: Improved Design and Analysis

CHAOUKI HANNACHI, (Member, IEEE), AND SERIOJA OVIDIU TATU, (Senior Member, IEEE)
Institut National de la Recherche Scientifique, Centre Énergie, Matériaux et Télécommunications, Montréal, QC H5A1K6, Canada

Corresponding author: Chaouki Hannachi (hannachi@emt.inrs.ca)

This work was supported in part by the National Science Engineering Research Council of Canada and in part by the Centre de Recherche en Électronique Radiofréquence of Montréal through the Fonds de recherche du Quebec–Natures et technologies.

ABSTRACT In this paper, a broadband 60-GHz millimeter-wave 4 × 1 microstrip patch antenna array using the gap-coupled technique is presented and analyzed. In order to meet the challenging requirement of reduced size related to this kind of technique, and facilitate the integration with other integrated passive or active devices, the proposed antenna array has been designed on a thin ceramic substrate ($\varepsilon_r = 9.9$ and $h = 127\ \mu$m), using an miniature hybrid microwave integrated circuits (MHMIC) fabrication process. The proposed structure is based on a modified shape of a gap-coupled patch element with curved radiating edges. For further analysis, the performances of the latter in terms of impedance bandwidth, gain, and radiation efficiency were investigated and compared with a conventional structure of a rectangular gap-coupled patch antenna. The obtained results clearly show that the proposed gap-coupled array structure provides an improved bandwidth (7%) and an enhanced gain (10.7 dB), while maintaining a reduced size (5.2 mm × 9.5 mm). All these benefits make it an attractive candidate for the future integrated millimeter-wave RF front-end circuits; it can, however, be connected directly to various MHMIC passive circuits, or active devices through using the wire bonding technology, on a standard thin-film alumina substrate.

INDEX TERMS Broadband, gap-coupling, microstrip antenna arrays, millimeter-wave, patch antennas, 60 GHz.

I. INTRODUCTION

Recently, printed antennas for millimeter-wave applications have become an increasingly important topic given the attractive features such as low profile, light weight, low manufacturing cost, and ease of fabrication and integration with Miniature Hybrid Microwave Integrated Circuits (MHMICs) or Microwave Monolithic Integrated Circuits (MMICs). They have become key components for many various commercial, industrial, and military applications including aircraft, spacecraft, satellite, missiles, cars, and even handheld mobile telephones [1]. Despite its many advantages, the general design of the microstrip patch antenna usually suffers from its intrinsic narrow bandwidth, which is of the order of a few percent (2% - 5%). This characteristic constitutes a real limitation in most of the wireless communication systems that are increasingly designed to support a large number of users and to provide high data-rate information [2].

In order to overcome this constraint, various techniques were adopted to increase the bandwidth of microstrip patch antennas, such as the slot-loading technique, the multilayered technique, the stacked multilayered technique and the use of modified or partial ground [3]–[10]. However, their implementation in practice further complicates the fabrication process, and may pose a difficulty in terms of integration with the existing planar fabrication processes. Many other approaches related to the substrate material choices have also been proposed for enhancing the bandwidth, for instance, by increasing the electrical thickness of the substrate, or by reducing the dielectric constant. Indeed, the increase in substrate thickness significantly degrades the antenna efficiency, especially at millimeter-wave frequencies because of surface wave effects; on the other hand, there are practical limitations in decreasing the dielectric constant [2].

The technique of gap-coupled multiple resonators used in microstrip antenna structures, is among the most promising techniques, and the simple solutions have proven to significantly increase operational bandwidth and antenna gain [11]–[14]. They have been subject to numerous researches over the past years, but, nonetheless, the vast majority of them have brought more interest for low-frequency antenna structures [11]–[20]. Therefore, they do not consider the same issues as in millimeter-wave

frequencies, particularly at 60 GHz band. In fact, at this frequency band, the surface wave propagations and the high mutual coupling between adjacent elements have a severe impact on the antenna radiation performance. Moreover, signals are additionally attenuated (10-17 dB/km) due to oxygen absorption, besides the inherent very high path loss caused by the operating frequency. This restricts the use of 60 GHz band for long distance communication (>2 km), and hence makes it entirely suitable for short-range wireless communications (several meters for low power to max 1 km for backhaul solutions) [21]–[23]. The frequency reuse is, therefore, one of the main advantages. Nevertheless, these drawbacks can be limited by designing antennas with a high efficiency, high gain, an acceptable bandwidth, and readily expandable to compact array configurations.

In this paper, a compact broadband 4 × 1 millimeter-wave microstrip patch antenna array using the gap-coupled technique is designed, fabricated, and analyzed. The proposed structure is based on gap-coupled microstrip patch elements having curved radiating edges. The idea is to maintain an optimized coupling level from the driven to the parasitic element through the modification of the current flowing way around the patch edges. This approach could significantly enhance the operational bandwidth, as compared to the common rectangular gap-coupled structure. For performance comparison, an equivalent rectangular gap-coupled patch antenna was also designed as a reference antenna. In order to enable a compact size that usually constitutes a major problem in this kind of technique, an MHMIC fabrication process, and a thin ceramic substrate with a high dielectric constant ($\varepsilon_r = 9.9$, $h = 127$ μm) have been employed. Finally, to investigate the coupling effect of the gap on the proposed gap-coupled structure, parametric studies were conducted to enable a gap width and input impedance matching optimization.

II. ANTENNA DESIGNS, FABRICATION, AND MEASUREMENTS

In order to point out the usefulness of the proposed gap-coupled structure in the optimization of the coupling between the driven patch and the parasitic element, a conventional rectangular microstrip patch antenna is used as reference antenna for performance comparison. Therefore, a consistent comparison between the single rectangular patch (SRP) and the single modified patch (SMP) antenna, as well as between their associated gap-coupled configurations is performed. For that purpose, the Advanced Design System (ADS) software of Keysight Technologies is used for circuit design, simulation, and parameter optimization. As a manufacturing technique, a standard MHMIC fabrication process on a thin ceramic substrate has been adopted. The latter provides several interesting features, including miniature circuits, low costs, as well as high level of integration and the use of high-precision thin film resistors, fabricated with microstrip line, such as in the case of our fabricated gap-coupled array prototype.

The geometrical configurations of the optimized single modified patch (SMP) and its equivalent single rectangular patch (SRP) antenna are shown in Fig. 1. Their physical parameters are: $W = 2R = 1.071$, $L = 0.731$, $W_0 = 0.708$, $L_1 = 0.266$, $L_2 = 0.307$, $d = 0.411$, $d_1 = 0.231$, $d_2 = 0.180$, $e = e_1 = 0.061$, $e_2 = 0.093$, $W_1 = W_2 = 0.127$, $D = 0.660$, $f = 0.058$, $f_1 = 0.078$, $E = 0.152$, all units being millimeters.

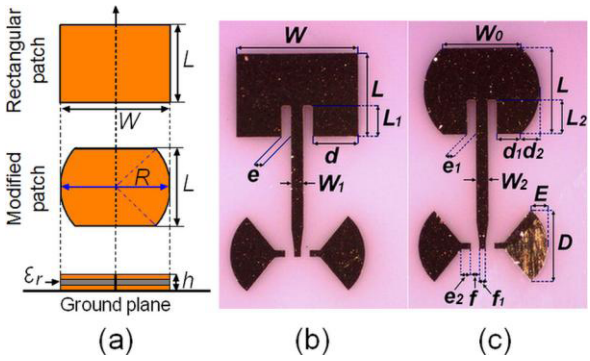

FIGURE 1. Single modified patch antenna and its equivalent rectangular patch in (a) Photograph of the fabricated prototypes with the geometrical parameters of the single rectangular patch antenna, and the single modified patch antenna in (b), and (c) respectively.

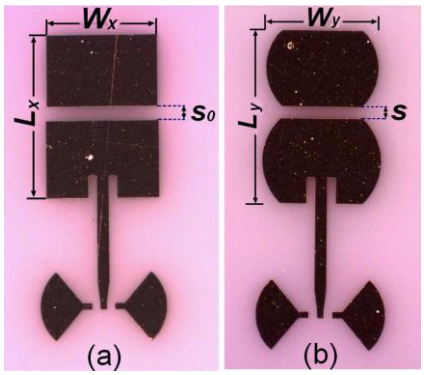

FIGURE 2. Photograph of the fabricated prototype with the geometrical parameters of (a) the rectangular gap-coupled microstrip patch antenna and (b) the modified gap-coupled microstrip patch antenna.

The rectangular gap-coupled patch antenna (RGCP) and the modified gap-coupled patch (MGCP) in Fig. 2 are also designed to achieve better control of the coupling between the driven patch and the parasitic element through optimization of the resonating lengths and the gap width between them. Accordingly, a larger operational bandwidth and the best input impedance matching will be achieved. Their optimized geometrical parameters are: $W_x = 1.036$, $L_x = 1.516$, $s_0 = 0.111$, $W_Y = 1.036$, $L_Y = 1.564$, $s = 0.101$, all units being millimeters.

The on-wafer return loss measurements of all fabricated microstrip antenna structures were performed using a Cascade Microtech probe station equipped with GSG 150 μm coplanar probes. The latter is connected to a Keysight (Agilent) Technologies millimeter-wave network analyzer (E8362B), with E-band extension modules, operating in 60 – 90 GHz band. Therefore, a coplanar line (CPWG) to

microstrip transition is designed and fabricated to enable an input return loss measurement with GSG 150 μm coplanar probes. Quarter-wavelength open circuited lines and sectors were also employed as millimeter-wave RF short-circuits while avoiding via holes to ensure measurement repeatability and accuracy. This feeding method is selected because it is the most appropriate, in view of the very compact size of the proposed microstrip structures, and the fragility of the ceramic alumina substrate ($h = 127$ μm, and a very thin gold layer metallization of 1 μm). This makes the implementation of a standard 1.85 mm V-connector very challenging, and may even further complicate the fabrication process. In order to ensure an accurate measurement, the on-wafer Through Reflect Line (TRL) calibration technique was also adopted using the calibration kit on the same ceramic alumina substrate as the devices under test (DUT) [24], [25].

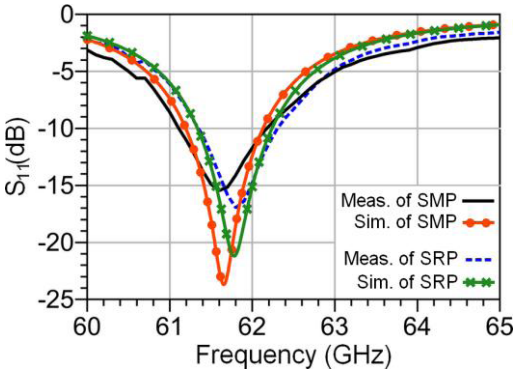

FIGURE 3. Measured and simulated return loss of the single modified patch (SMP) and the single rectangular patch antenna (SRP).

Fig. 3 compares the simulated and measured return losses of the single modified patch (SMP) and its equivalent single rectangular patch (SRP) antenna. As it can be seen, the starting frequency is 60 GHz instead of 57 GHz (the starting frequency of unlicensed 60 GHz frequency band). This is due to the capability of our on-wafer measurement facility, as described earlier. Accordingly, the proposed microstrip antenna structures were designed to operate at 61.6 GHz to enable performance comparison. It should be noted that these structures are easily scalable with frequency, such as in the case of the proposed 4 × 1 modified gap-coupled antenna array, which was designed to operate at the unlicensed frequency range around 60 GHz.

The obtained return loss results in Fig. 3 show a good agreement with each other over the considered frequency band, from 60 to 65 GHz. The measured impedance bandwidth at −10 dB of the single modified patch (SMP) covers the frequency range of about 1.1 GHz, from 61.1 to 62.2 GHz, which represents 1.78 % at the center frequency of 61.6 GHz. The single rectangular patch (SRP) antenna shows almost the same measured return loss performances with approximately 1 GHz of the measured impedance bandwidth, from 61.4 to 62.4, representing 1.62 % at 61.6 GHz.

Fig. 4 shows the measured return loss as compared with the simulated one over the investigated frequency band

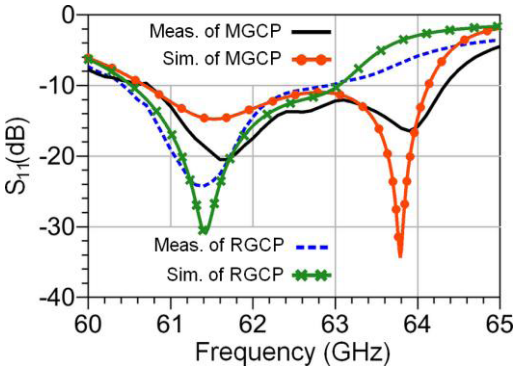

FIGURE 4. Measured and simulated return loss of the modified gap-coupled patch (MGCP) and the rectangular gap-coupled patch antenna (RGCP).

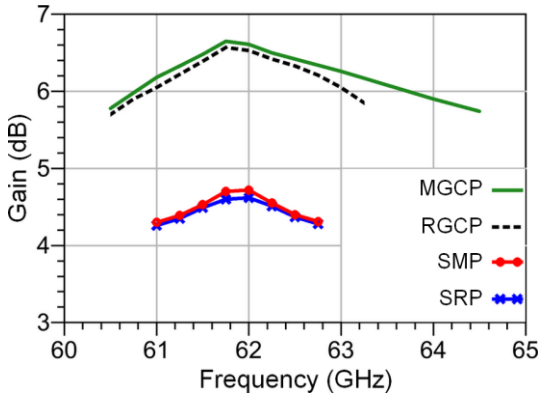

FIGURE 5. Calculated gain at −10 dB bandwidth of the single modified patch (SMP), the single rectangular patch antenna (SRP), the modified gap-coupled patch (MGCP) and the rectangular gap-coupled patch antenna (RGCP).

(60 to 65 GHz) for the modified gap-coupled patch (MGCP) and the rectangular gap-coupled patch antenna (RGCP). As it can be seen from Fig. 4, the comparison between the measured and the simulated insertion loss showed very good agreement. The modified gap-coupled patch (MGCP) resonates efficiently at 61.6 GHz and 63.9 GHz, with a measured impedance bandwidth of 3.7 GHz, from 60.7 to 64.4 GHz, representing, 5.92 % at the center frequency of 62.5 GHz.

The rectangular gap-coupled patch antenna (RGCP) can reach a measured impedance bandwidth of 2.6 GHz (4.16% at the center frequency of 62.5 GHz), from 60.4 to 63 GHz, which is clearly 1.1 GHz less than the measured bandwidth obtained previously in the modified gap-coupled patch (MGCP).

However, a slight resonant frequency shift between the simulated and the measured return loss is observed for both structures, which is mainly due to the tolerances of the dielectric constant and thickness of the ceramic substrate, substrate losses, and fabrication tolerances.

In order to investigate the impact of the proposed single and gap-coupled configurations in Figs. 1(c) and Fig. 2(b) on gain and efficiency, a comparative study at the operating frequency bands (−10 dB return loss bandwidth) is carried out. For that purpose, the single rectangular patch antenna (SRP) and the rectangular gap-coupled patch antenna (RGCP)

in Figs. 1(b) and Fig. 2(a) are considered as reference antennas for performance comparison. In Fig. 5, we can see the calculated maximum gain versus the frequency of the single modified patch (SMP), the single rectangular patch antenna (SRP), the modified gap-coupled patch (MGCP) and the rectangular gap-coupled patch antenna (RGCP), respectively. As it can be seen from the figure, the gain of the single modified patch (SMP) and of the single rectangular patch antenna (SRP) are in close agreement. They increase from 4.25 dB (at 61 GHz) to 4.7 dB (at 62 GHz), and after that they decrease to achieve again 4.25 dB at 62.8 GHz. Similarly, for the modified gap-coupled patch (MGCP) and the rectangular gap-coupled patch antenna (RGCP). They are very close together over 2 GHz, from 60.5 to 62.5 GHz, with peak gains of 6.62 and 6.55 dB, respectively. However, the modified gap-coupled patch (MGCP) antenna shows a slightly higher gain as compared to the rectangular gap-coupled patch antenna (RGCP). It achieves more than 5.6 dB in the frequency range of 60.5 to 64.5 GHz, whereas the rectangular gap-coupled patch antenna (RGCP) reaches the same level of performance in only 2.7 GHz of frequency range, from 60.5 to 63.2 GHz.

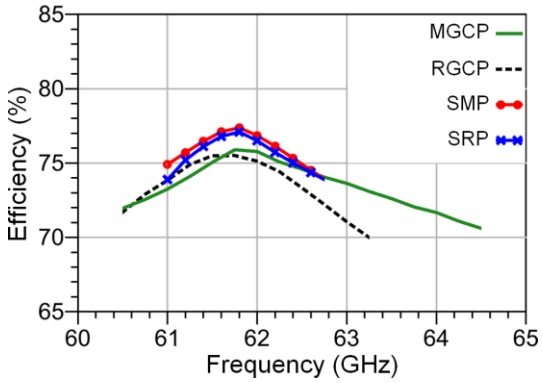

FIGURE 6. Calculated efficiency at −10 dB bandwidth of the single modified patch (SMP), the single rectangular patch antenna (SRP), the modified gap-coupled patch (MGCP) and the rectangular gap-coupled patch antenna (RGCP).

The calculated radiation efficiency for all configurations is shown in Fig 6. As it can be observed, the radiation efficiency variations of the single modified patch (SMP) and the single rectangular patch (SRP) antenna are very close one to another. The maximum value reached for both is 77% at 61.8 GHz, whereas the minimum value achieved is around 73.5% at 61 and 62.75 GHz, respectively. For the gap-coupled structures, we can see that the modified gap-coupled patch (MGCP) provides better efficiency, over 70% of the entire operating frequency band, from 60.5 to 64.5 GHz. However, the same performance is obtained for the rectangular gap-coupled patch antenna (RGCP), in only 2.7 GHz of the operating frequency band, from 60.5 to 63.2 GHz.

III. THEORETICAL ANALYSIS

The proposed modified gap-coupled patch (MGCP) structure can be analyzed for the two modes, commonly known as even and odd. The theory of such structures has recently been well

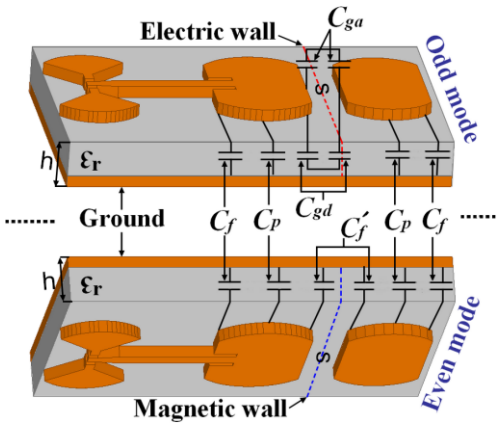

FIGURE 7. Even and odd mode capacitances of the proposed gap-coupled microstrip patch antenna structure.

investigated in literature [11], [26]. However, this structure can be analyzed by adopting the theory of coupled microstrip lines and coupled microstrip antenna. In this analysis, the total capacitance of the coupled structure is taken as the parallel plate capacitance (C_p) and two fringing capacitances (C_f, C_f') for both even and odd mode. It should be noted that the additional fringing capacitance at the adjacent edge of the patches is in fact the result of the additional parasitic element in the proposed gap-coupled microstrip patch structure. Fig. 7 shows in detail all those capacitances for both modes, even and odd, respectively.

TABLE 1. Even and odd mode capacitance equations.

Even-mode capacitance	Odd-mode capacitance
$C_{even} = C_P + C_f + C_f'$	$C_{odd} = C_P + C_f + C_{gd} + C_{ga}$
$C_P = \varepsilon_r \varepsilon_0 (w/h)$ (1)	
$C_f = \frac{1}{2}\left[\frac{\sqrt{\varepsilon_{eff}}}{cZ_C - C_P}\right]$ (2)	
$C_f' = C_f\left[1 + A\left(\frac{h}{s}\right)\tanh\left(\frac{10s}{h}\right)\right]^{-1}\left(\frac{\varepsilon_r}{\varepsilon_{eff}}\right)^{1/2}$ (3)	
$A = \exp\left(-0.1\exp\left(2.33 - 2.53\, w/h\right)\right)$ (4)	
$C_{gd} = \left(\frac{\varepsilon_0 \varepsilon_r}{\pi}\right)\ln\left[\coth\frac{\pi s}{4h}\right] + 0.65 C_f\left[\frac{0.02}{(s/h)}\sqrt{\varepsilon_r} + 1 - \frac{1}{\varepsilon_r^2}\right]$ (5)	
$C_{ga} = \frac{1}{2}K(k')\frac{\varepsilon_0}{K(k)}$ (6)	
$k = \frac{s/h}{(s/h) + 2(w/h)}$, $k' = \sqrt{1 - k^2}$ (7)	

The values of these capacitances can be expressed in terms of even and odd mode parameters for propagation, as illustrated in Table 1 [11], [26].

From the table, it is noted that the expressions for the capacitances cited earlier including C_p, C_f, and C_f' are given in (1), (2), and (3), respectively. We can also distinguish two other capacitances that characterize the coupling effect between the fed patch and the parasitic patch in the odd mode.

The first one is the dielectric coupling capacitance C_{gd}, which represents the capacitance value due to the electric flux in the dielectric area, where its value is calculated in (5). The second one is the air coupling capacitance C_{ga}, which describes the gap capacitance in air. Its value can be obtained from (6), where K (k) and K (k') designate the elliptic function and its complement (7).

In this analysis, particular attention is paid to the coupling effect between the driven element and the parasitic one. However, according to Table 1, this effect can be assessed quantitatively by estimating the values of the dielectric coupling capacitance C_{gd} and the air coupling capacitance C_{ga}, for different normalized gap distances s/h. The obtained results for those capacitances with the employed alumina substrate are shown in Fig. 8.

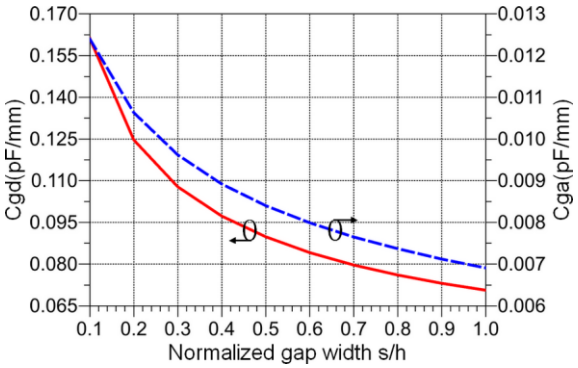

FIGURE 8. Coupling capacitances versus normalized gap width (s/h) for the alumina substrate ($\varepsilon_r = 9.9$ and $h = 127$ μm).

It is noteworthy that the normalized gap width used to obtain the results is increased every step by 0.1 (one-tenth of the substrate height h), reaching a maximum value of 1, which corresponds to an overall increase of one time the substrate height h ($s = h$). In view of these considerations, it can be seen that as the gap width increases, the coupling effect decreases for both capacitances, C_{gd} and C_{ga}. The dielectric coupling capacitance C_{gd} and the air coupling capacitance C_{ga} have reached their maximum values at 0.162 pF/mm and 0.0125 pF/mm respectively, for s/h = 0.1, whereas the minimum values reached by these capacitances are 0.072 pF/mm and 0.0069 pF/mm respectively, for $s/h = 1$. These results clearly demonstrate that the variations of the dielectric coupling capacitance C_{gd} are approximately ten times higher than the variations of the air coupling capacitance C_{ga}. This may be explained by the high relative dielectric constant ($\varepsilon_r = 9.9$) and low thickness ($h = 127$ μm) of the used alumina substrate.

In order to determine the optimum value of the gap distance allowing for a better input impedance matching, the variation of the latter has been expressed as a function of frequency for different normalized gap distances at Fig. 9. It is observed that the input impedance increases with the increase of the gap distance at 60 GHz, and then it decreases, to attain a minimum value of 20 Ω at the frequency range of 64 to 65 GHz. Different resonance peaks are also observed at the frequency

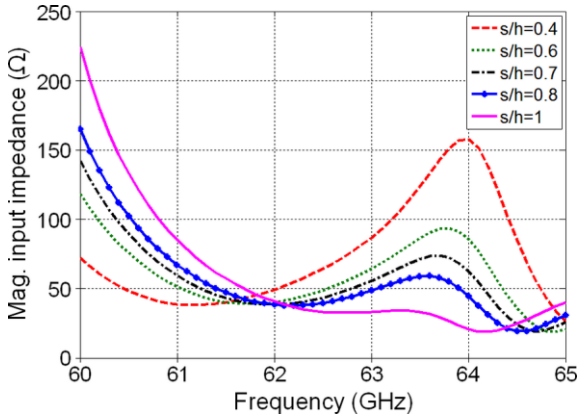

FIGURE 9. Variation of the input impedance magnitude with frequency for different normalized gap distances.

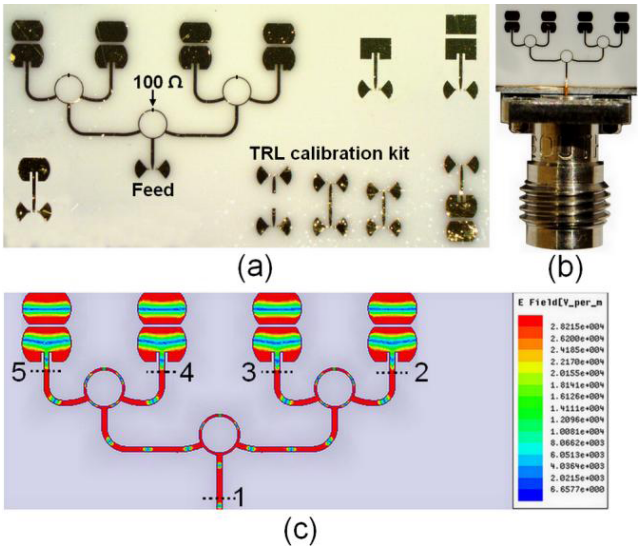

FIGURE 10. Photographs of the fabricated 4 × 1 gap-coupled antenna array (a) prototype with a coplanar line (CPWG) to microstrip transition (b) prototype with a V-connector (1.85) mm and (c) simulated surface current distributions on the conductor.

around 63.8 GHz, which increase with the decrease of the gap distance, to reach a maximum value of 160 Ω. Overall, the optimum value of the gap distance allowing a proper input impedance matching over the considered frequency band corresponds to the normalized value of $s/h = 0.8$ (value selected for our design).

IV. MODIFIED 4 × 1 GAP-COUPLED MICROSTRIP ANTENNA ARRAY

The fabricated prototypes of the proposed 4 × 1 modified gap-coupled antenna array with coplanar line (CPWG) to microstrip transition and V-connector (1.85 mm), are shown in Figs. 10 (a) and (b), respectively. Its structure consists of four modified gap-coupled patch elements, spaced about $0.55\lambda_o$ ($\lambda_o = 5$ mm), and a parallel feed network composed of three rounded shape Wilkinson power dividers/combiners [27], along with the 50 Ω transmission

lines. It should be noted that this kind of feed network often employs only T-junction power dividers. Therefore, the architecture of the latter has a decisive effect on the performance of the microstrip antenna arrays. In this context, the Wilkinson power divider/combiner was selected as the preferred solution to the lossless T-junction problems, which is not matched at all ports and not isolated between output ports. Furthermore, the employed rounded shape Wilkinson power divider/combiner has recently proven that it can achieve the ideal three-port network properties including lossless, reciprocal, and matching at all ports, at millimeter-wave frequencies (up to 86 GHz) [28]. This is the reason why we opted for the rounded shape Wilkinson divider as the best choice in our optimized design of the parallel feed network.

In order to understand the excitation mechanism of the 4×1 modified gap-coupled antenna array, simulated surface current distributions on the conductor are illustrated in Fig. 10(c). In this figure, the electrical field is uniformly distributed, and is coupled from the driven elements to the parasitic elements, which results in excitation of all patches. It should also be mentioned that this coupling is mainly governed by the gap thickness and patch widths between driven and parasitic elements.

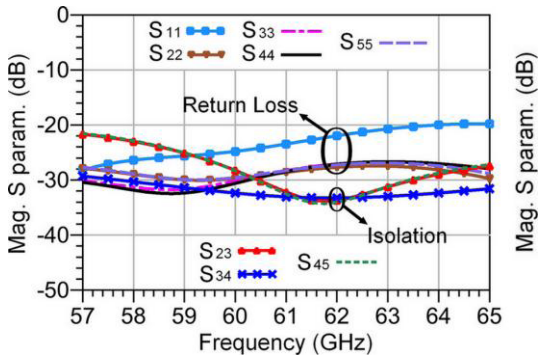

FIGURE 11. Simulated RF input return loss and isolation of the feed network.

Furthermore, to estimate losses and assess the performance of the proposed parallel feed network, its simulated S-parameters including the return loss, isolation and the transmission coefficient are also presented in Figs. 11 and 12, respectively.

Fig. 11 shows the simulated S-parameters of the return loss and the output isolation of the employed feed network according to Fig. 10 (c) above. These results demonstrate a good matching at all ports, with more than -20 dB over the entire unlicensed frequency band, from 57 to 64 GHz. The isolation factor between the adjacent ports (2-3, 3-4, and 4-5) at the output is at least 20 dB, and it has reached 33 dB around 61.8 GHz. This high isolation level is indeed the result of the integrated high-precision resistor implemented with accuracy on a 100 Ω per square titanium oxide thin layer [27], using the Miniature Hybrid Microwave Integrated Circuit (MHMIC) technology (see Fig. 10 (a)).

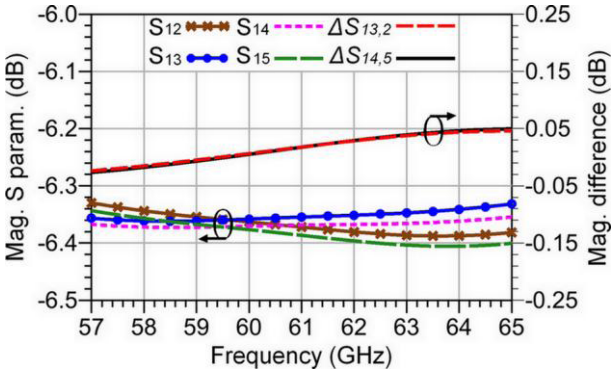

FIGURE 12. Simulated transmission S-parameter magnitudes of the feed network.

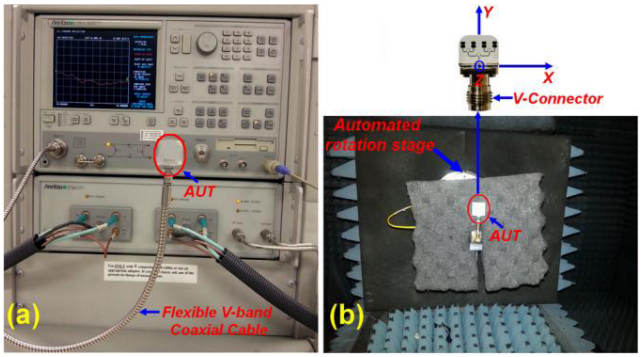

FIGURE 13. Antenna under test (AUT) with: (a) The Anritsu 37397C vector network analyzer (VNA). (b) The automated anechoic chamber.

The simulated transmission coefficient results, S_{12} to S_{15}, according to the ports at Fig. 10 (c) are illustrated in Fig. 12. These results show less than 0.5 dB of additional insertion loss over the whole 57 to 65 GHz frequency band. However, quasi-null amplitude imbalances $\Delta S_{13,2}$ and $\Delta S_{14,5}$ between the requested ports are obtained, which do not exceed 0.15 dB. These results prove that the designed feed network is well optimized and has almost negligible additional losses.

In order to ensure complete characterization of the proposed gap-coupled antenna array configuration, a 1.85 mm V-connector from Southwest Microwave Company was used to perform measurements of radiation pattern and return losses over the entire unlicensed 60-GHz frequency band (57 - 65 GHz). For this purpose, an Anritsu 37397C vector network analyzer (40 MHz - 65 GHz), and an automated far-field antenna measurement system (up to 110 GHz) composed of a rotating standard horn antenna (Quinstar, Model n°qwh-vprr00) have been employed. Photos of both facilities, including the measurement set-ups are shown in Fig. 13.

The return loss measurements (1.85 mm V-connector and on-wafer measurements) have been performed after standard TRL calibration of the Vector Network Analyzers (VNAs). The obtained results were compared with the simulations in Fig. 14, over the considered frequency ranges, from 57 to 64 GHz for the 1.85 mm V-connector measurement, and from 60 to 64 GHz for the on-wafer measurement. These results show that the proposed 4×1 modified

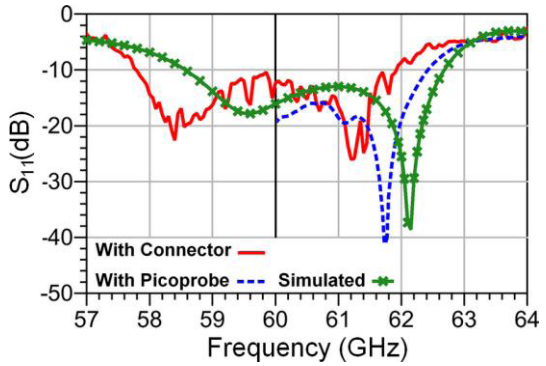

FIGURE 14. Measured and simulated return loss of the fabricated 4 × 1 gap-coupled antenna arrays.

gap-coupled antenna array at −10 dB has a measured bandwidth of 4.2 GHz, from 57.8 to 62 GHz, which represents a measured bandwidth of 7 % at the center frequency of 60 GHz. This trend is also confirmed for the on-wafer return loss measurement from 60 to 64 GHz.

Globally, simulated and measured results are in reasonable agreement over the whole 57 to 65 GHz frequency band, except for a small frequency shift at resonant frequencies, not exceeding 1 GHz. The resonant frequency from simulation is at 59.5 and 62.2 GHz, from measurement at 58.4 and 61.2 GHz (1.85 mm V-connector measurement), whereas from the on-wafer measurement, at around 61.8 GHz. This is probably caused by the fabrication tolerance, uncertainties in material parameters, and measurement imperfections.

As it can be seen from the Fig. 14 above, the measured return loss using the 1.85 mm V-connector contains some additional amplitude ripples over the considered frequency band (57-65 GHz). This is primarily a result of the unwanted reflections because of the mismatch effects between the 50 Ω microstrip feed line and the connector, which are in turn related to the soldering quality of the V-connector with the 50 Ω microstrip feed line.

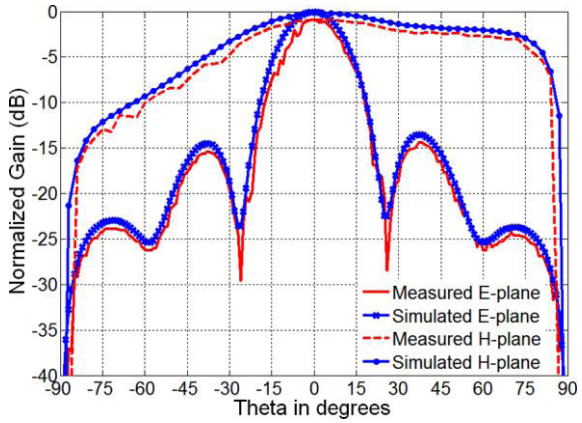

FIGURE 15. Radiation patterns of the fabricated 4 × 1 gap-coupled antenna array in E and H-planes at 60 GHz.

The simulated and measured radiation patterns at 60 GHz in both E and H-planes are presented in Fig. 15 below.

The simulated and measured E-plane patterns are in agreement, while maintaining high symmetry and a good broadside radiation pattern. However, a certain asymmetry in the H-plane pattern is observed, which is mainly related to the parasitic elements coupling that makes the radiation pattern slightly inclined towards the front of the array. The half-power beamwidths (HPBW) in the E-plane and H-plane are 15° and 91° respectively, and the first side lobe is about 13.46 dB below the main lobe.

The small variations observed between the simulated and the measured results for both planes in Fig. 15 are probably caused by the connector losses during radiation pattern measurement and fabrication tolerances, as mentioned earlier.

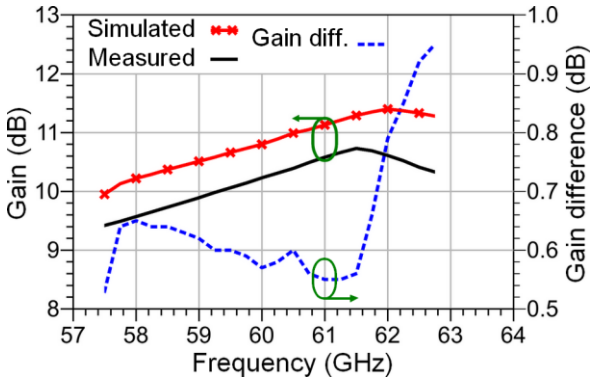

FIGURE 16. Simulated and measured gains of the fabricated 4 × 1 gap-coupled antenna array.

The results of the measured and simulated peak gain of the proposed 4 × 1 gap-coupled array configuration over the frequency band of 57.5 to 62.8 GHz (at the operating frequency bands) are shown in Fig. 16.

These results show more than 10 dB of measured gain in the operating frequency range (−10 dB return loss bandwidth), from 57.8 to 62 GHz with a maximum measured peak of 10.7 dB at 61.5 GHz (simulated 11.4 dB at 62 GHz). However, the difference between the simulated and the realized gain is more or less 0.95 dB in the considered frequency band. As mentioned previously, most of this loss is due to the additional reflections resulted from the 1.85 mm (V) connector, which can reach the insertion loss of 1 dB below 67 GHz [29]. In fact, this problem can possibly be avoided given the miniature size of the antenna (it does not exceed 5.2 mm by 9.5 mm) which enables it to be easily integrated with other components in the package.

V. CONCLUSION

In this study, an improved gap-coupling concept for 60 GHz millimeter-wave microstrip patch antennas has been theoretically investigated, and experimentally validated. For this purpose, a new compact configuration of a gap-coupled patch antenna having curved radiating edges has been designed, fabricated, and tested. The principle is to maintain an optimized coupling level from the driven to the parasitic element through the modification of the current flowing way around

the edges of the patches. This approach may enhance the operational bandwidth to more than four times and increases the gain up to 3 dB as compared to the single modified patch.

Based on the modified gap-coupled patch (MGCP) antenna element that has proved a better bandwidth performance as compared to the rectangular gap-coupled patch (RGCP) structure, a 4 × 1 gap-coupled array antenna has been also designed and fabricated. The obtained results in terms of bandwidth (7 %), gain (10.7 dB), and compact size (5.2 mm by 9.5 mm), obviously prove a high optimization level of the proposed structure and make it a serious candidate for integration in the future broadband millimeter-wave integrated circuits.

REFERENCES

[1] C. A. Balanis, *Antenna Theory Analysis and Design*, 3rd ed. New York, NY, USA: Wiley, 2011.
[2] G. Kumar and K. P. Ray, *Broadband Microstrip Antennas*, Boston, MA, USA: Artech House, 2003.
[3] S. Liu, W. Wu, and D. G. Fang, "Single-feed dual-layer dual-band E-shaped and U-slot patch antenna for wireless communication application," *IEEE Antennas Wireless Propag. Lett.*, vol. 15, pp. 468–471, 2016.
[4] H. Wong, K. K. So, and X. Gao, "Bandwidth enhancement of a monopolar patch antenna with V-shaped slot for car-to-car and WLAN communications," *IEEE Trans. Veh. Technol.*, vol. 65, no. 3, pp. 1130–1136, Mar. 2016.
[5] X. Zhang and L. Zhu, "Gain-enhanced patch antennas with loading of shorting pins," *IEEE Trans. Antennas Propag.*, vol. 64, no. 8, pp. 3310–3318, Aug. 2016.
[6] H. W. Lai, D. Xue, H. Wong, K. K. So, and X. Y. Zhang, "Broadband circularly polarized patch antenna arrays with multiple-layers structure," *IEEE Antennas Wireless Propag. Lett.*, vol. 16, pp. 525–528, 2017.
[7] W. C. Yang, H. Wang, W. Q. Che, Y. Huang, and J. Wang, "High gain and low-loss millimeter-wave LTCC antenna array using artificial magnetic conductor structure," *IEEE Trans. Antennas Propag.*, vol. 63, no. 1, pp. 390–395, Jan. 2015.
[8] H. Sun, Y.-X. Guo, and Z. Wang, "60-GHz circularly polarized U-slot patch antenna array on LTCC," *IEEE Trans. Antennas Propag.*, vol. 61, no. 1, pp. 430–435, Jan. 2013.
[9] R. Florencio, R. R. Boix, and J. A. Encinar, "Fast and accurate MoM analysis of periodic arrays of multilayered stacked rectangular patches with application to the design of reflectarray antennas," *IEEE Trans. Antennas Propag.*, vol. 63, no. 6, pp. 2558–2571, Jun. 2015.
[10] R. Azim, M. T. Islam, and N. Misran, "Ground modified double-sided printed compact UWB antenna," *Electron. Lett.*, vol. 47, no. 1, pp. 9–11, Jan. 2011.
[11] C. K. Aanandan, P. Mohanan, and K. G. Nair, "Broad-band gap coupled microstrip antenna," *IEEE Trans. Antennas Propag.*, vol. 38, no. 10, pp. 1581–1586, Oct. 1990.
[12] A. Kandwal and S. K. Khah, "A novel design of gap-coupled sectoral patch antenna," *IEEE Antennas Wireless Propag. Lett.*, vol. 12, pp. 674–677, 2013.
[13] G. Kumar and K. Gupta, "Broad-band microstrip antennas using additional resonators gap-coupled to the radiating edges," *IEEE Trans. Antennas Propag.*, vol. 32, no. 12, pp. 1375–1379, Dec. 1984.
[14] P. Kumar and G. Singh, "Gap-coupling: A potential method for enhancing the bandwidth of microstrip antennas," *Adv. Comput. Techn. Electromagn.*, vol. 2012, 2012, Art. no. 00110.
[15] C. Wood, "Improved bandwidth of microstrip antennas using parasitic elements," *IEE Proc. H Microw., Opt. Antennas*, vol. 127, no. 4, pp. 231–234, Aug. 1980.
[16] Q. Song and X. X. Zhang, "A study on wideband gap-coupled microstrip antenna arrays," *IEEE Trans. Antenna Propag.*, vol. 43, no. 3, pp. 313–317, Mar. 1995.
[17] C. K. Wu and K. L. Wong, "Broadband microstrip antenna with directly coupled and parasitic patches," *Microw. Opt. Technol. Lett.*, vol. 22, pp. 348–349, Sep. 1999.
[18] K. P. Ray, S. Ghosh, and K. Nirmala, "Compact broadband gap-coupled microstrip antennas," in *Proc. IEEE Antennas Propag. Soc. Int. Symp.*, vols. 9–14. Jul. 2006, pp. 3719–3722.
[19] P. Nayeri, F. Yang, and A. Z. Elsherbeni, "Bandwidth improvement of reflectarray antennas using closely spaced elements," *Prog. Electromagn. Res. C*, vol. 18, pp. 19–29, Nov. 2011.
[20] A. A. Deshmukh and K. P. Ray, "Broadband proximity-fed square-ring microstrip antennas," *IEEE Antennas Propag. Mag.*, vol. 56, no. 2, pp. 89–107, Apr. 2013.
[21] W. Yang, K. Ma, K. S. Yeo, and W. M. Lim, "A compact high-performance patch antenna array for 60-GHz applications," *IEEE Antennas Wireless Propag. Lett.*, vol. 15, pp. 313–316, 2016.
[22] C. Hannachi and S. O. Tatu, "A new compact V-band six-port down-converter receiver for high data rate wireless applications," in *Proc. IEEE Topical Conf. Wireless Sensors Sensor Netw. (WiSNet)*, San Diego, CA, USA, Jan. 2015, pp. 26–28.
[23] A. Adane, F. Gallée, and C. Person, "Bandwidth improvements of 60GHz micromachining patch antenna using gap coupled U—Microstrip feeder," in *Proc. 4th Eur. Conf. Antennas Propag.*, Barcelona, Spain, Apr. 2010, pp. 1–5.
[24] C. Hannachi, D. Hammou, T. Djerafi, Z. Ouardirhi, and S. O. Tatu, "Complete characterization of novel MHMICs for V-band communication systems," *J. Electr. Comput. Eng.*, vol. 2013, Oct. 2013, Art. no. 686708.
[25] C. Hannachi, E. Moldovan, Z. Ouardirhi, and S. O. Tatu, "V-band six-port quadrature demodulator: Error vector magnitude analysis," in *Proc. 8th Global Symp. Millim. Waves (GSMM)*, Montreal, QC, Canada, May 2015, pp. 1–3.
[26] B. K. Kanaujia and A. K. Singh, "Analysis and design of gap-coupled annular ring microstrip antenna," *Int. J. Antennas Propag.*, vol. 2008, Jul. 2008, Art. no. 792123.
[27] D. Hammou, E. Moldovan, and S. O. Tatu, "Novel MHMIC novel MHMIC millimeter wave power divider/combiner," in *Proc. IEEE Can. Conf. Elect. Comput. Eng. (CCECE)*, May 2011 pp. 280–283.
[28] E. Moldovan and S. O. Tatu, "Design and characterization of novel W-band wide-band couplers and six-port circuit," in *Proc. Eur. Microw. Week, Conf.*, Paris, France, Sep. 2015, pp. 279–282.
[29] M. Hrobak, *Critical mm-Wave Components for Synthetic Automatic Test Systems*. Berlin, Germany, Springer Vieweg, Apr. 2015.

CHAOUKI HANNACHI (M'12) received the B.Sc. degree in electrical engineering from the University of Technology, Annaba, Algeria, in 2004, and the M.Sc. degree in electrical engineering from the University of Rouen, Rouen, France, in 2006, and the Ph.D. degree in telecommunications engineering from the Institut National de la Recherche Scientifique, Énergie Matériaux et Télécommunications, Montreal, QC, Canada, in 2017. He has been involved in a number of research projects as a member of Pervasive and Smart Wireless Applications for the Digital Economy Program, Energy Materials Telecommunications Research Center. His research interests include microwave/millimeter-wave applications design and characterization, antenna design, multi-port technologies, and millimeter-wave receiver front-ends for indoor wireless communications.

SERIOJA OVIDIU TATU (M'05–SM'13) received the B.Sc. degree in radio engineering from Polytechnic University, Bucharest, Romania, in 1989, and the M.A.Sc. and Ph.D. degrees in electrical engineering from the École Polytechnique of Montréal, Montreal, QC, Canada, in 2001 and 2004, respectively. He was with the National Company of Telecommunications, Rom-Telecom, Bucharest, where he was an RF Engineer and the Head of the Telecommunications Laboratory from 1989 to 1993, and the Technical Manager from 1993 to 1997. He is currently an Associate Professor with the Institut National de la Recherche Scientifique, Énergie Matériaux et Télécommunications, Montreal. His current research interests include microwave/millimeter-wave circuit design, hardware and software radio receivers, radar, and imaging systems.